2-I C3

THE RADIATION CHARACTERISTICS OF COINCIDENT INDEPENDENT APERTURES

by
B.A. Sichelstiel and D.K. Alexander

Westinghouse Electric Corporation
Systems Development Division
Baltimore, Maryland, USA

The use of two separate array antennas sharing the same frontal area leads to a new class of coincident apertures that uniquely offer full aperture gain and independent control of the radiated pattern characteristics. An experimental model of the concept was prepared using orthogonal superposition of two edge-slotted waveguide arrays. Single-axis electronic phasing was added to both arrays to permit independent steering of the two antenna beams. The excitation function of the front array was tapered to produce a low sidelobe radiation pattern and the measured results verify the computed scanning performance of the complete dual beam antenna system.

Introduction

In its simplest form, the dual independent beam antenna system uses two superimposed arrays having fixed, coincident radiated beams. The arrays may be comprised of colinear, interleaved, dielectric or ridge-loaded, H-plane slotted waveguides, or orthogonal E-plane slotted waveguides, or combinations of these waveguide configurations. Or, in a slightly more complex form, the pair of arrays may combine the use of dipoles or other radiating elements with waveguide. Ease of construction and the ability to mathematically model the arrays were considerations used in selecting the orthogonal E-plane slotted waveguide array configuration for the test model. The slots of the rear array, located at the spaces between the waveguides of the front array are "decoupled" from the front array by the orthogonal polarization characteristic of this design.

In the version described in this paper, an electronic beam steering feature has been added to increase the versatility of the technique. Without electronic beam steering the two beams are pointed together by gimballing the antenna assembly. Independent pointing control is accomplished by electronically steering each beam along one axis and mounting the complete unit on a two-axis gimbal. The combined steering methods will also permit much wider beam angle coverage. There is also the possibility of producing circularly polarized radiation with the nonelectronically scanned version by connecting the two arrays to a common terminal through proper time-quadrature phasing circuits.

Test Model Design

The radiating aperture of the model is approximately 21 inches square. Each array is made up of 27 edge-slotted waveguides. Each waveguide in the front array has 27 slots and in the rear array, 26. A waveguide manifold is used to end-feed each array. The rear array manifold is a conventional tee-junction type while the front array employs a unique variation of the directional coupler manifold.

The two arrays were designed to have quite different radiation characteristics. The front array is designed to have very low sidelobes, on the order of 40 dB down, with no more than 5-dB degradation during beam steering. The rear array has near maximum gain with first sidelobes only 16 to 18 dB down from the main beam.

The front array low sidelobe performance was accomplished through the use of a specially derived computer program which takes into account all mutual terms in the impedance matrix for the slot elements. The antenna was built directly from the computer generated dimensions and no adjustments were required to correct errors in design or construction. A number of design problems were encountered. Significant among them: (1) obtaining sufficiently high conductance values from the rear array slots, (2) matching the aperture of the rear array to free space, and (3) suppressing cross-polarized energy to acceptable levels.

The see-through space between the waveguides of the front array is determined by the element spacing of the front array and the height of the front array waveguide. Considering the near field environment of a typical slot in the rear array, we find two conducting walls, separated by this space immediately external to the slot. The impedance of the slot is significantly affected by the proximity of the walls. In addition, the radiated energy from the rear array experiences a step discontinuity as it passes through the plane of the front array face and enters free space. Left uncompensated, this discontinuity would

cause intolerable reflections.

The design used to solve both the above problems is shown in figure 1. The spacing of the metallic walls immediately external to the rear array slots has been increased allowing conductance values to be more than doubled. Treating this region and that between the front array waveguides as parallel plate waveguide, a quarter wavelength transformer is provided joining the two regions. In addition, dielectric strips are positioned and dimensioned to exactly cancel the energy reflected from the interface with free space. Both of these aperture matching techniques were designed to provide optimum performance for a broadside beam on the demonstration model. As beam steering takes place, their effectiveness decreases slightly.

Measured Performance

The measurements program on the test model was extensive but of particular interest were the following general goals: (1) obtaining very low sidelobe performance from the front array to match theoretically-derived patterns, (2) scanning the front array while maintaining low sidelobes, and (3) obtaining a predictable radiation pattern from the rear array. Looking first at the front array, figure 2 shows the H-plane pattern with sidelobes more than 40 dB down from the main beam peak. Peak sidelobe levels degrade slowly to about -34 dB at 34 degrees steering angle. At 39 degrees steering angle, a predicted grating lobe emerges.

The rear array produced broadside patterns of very regular and near-theoretical shape. As the rear antenna beam is steered, sidelobes rise slowly and gain falls evenly until a loss of about 3 dB is noted at 36 degrees steering angle.

Figure 3 shows gain degradation of the front array with steering angle. A less than 2-dB gain reduction is incurred at steering angles out to 35 degrees. Figure 4 shows peak sidelobe levels as the front array is steered. The investigation may be briefly summarized by comparing parameter goals with the values actually achieved (figure 5).

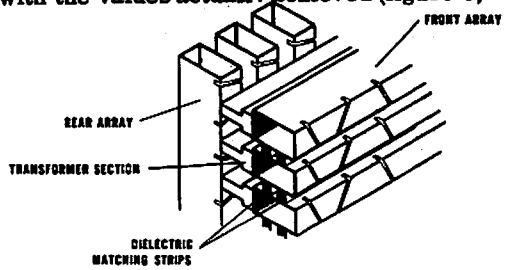

Figure 1. Array Face Detail

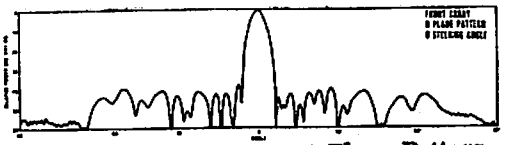

Figure 2. Front Array, H-Plane Pattern, 0° Steering Angle

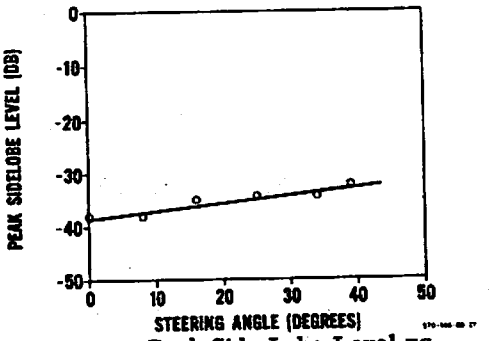

Figure 4. Peak Side Lobe Level vs Steering Angle

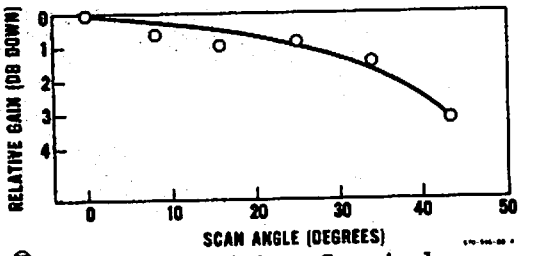

Figure 3. Gain vs Scan Angle

PARAMETER	FRONT ARRAY		REAR ARRAY	
	GOAL	ACTUAL	GOAL	ACTUAL
MAXIMUM STEERING ANGLE	45°	38°	45°	45°
PEAK SIDELOBE LEVEL				
BROADSIDE (-dB)	40	38	18	16
STEERED (-dB)	35	34	–	12
GAIN				
BROADSIDE (dB)	32.9	32.5	34.9	34.8
STEERED (dB)	31.4	31.0	–	30.8

Figure 5. Parameter Summary Table